TITLE HERE

by

JAMES SARTOR

A DISSERTATION

Presented to the Department of Physics
and the Division of Graduate Studies of the University of Oregon
in partial fulfillment of the requirements
for the degree of
Doctor of Philosophy

December 2021

DISSERTATION APPROVAL PAGE

Student: James Sartor

Title: ABSTRACT TITLE HERE

This dissertation has been accepted and approved in partial fulfillment of the requirements for the Doctor of Philosophy degree in the Department of Physics by:

Ben Mcmorran	Chair
Eric Corwin	Advisor
Jayson Paulose	Core Member
Marina Guenza	Institutional Representative

and

Andy Karduna	Interim Vice Provost for Graduate Studies

Original approval signatures are on file with the University of Oregon Division of Graduate Studies.

Degree awarded December 2021

DISSERTATION ABSTRACT

James Sartor

Doctor of Philosophy

Department of Physics

December 2021

Title: ABSTRACT TITLE HERE

abstract here

This dissertation includes previously published and unpublished coauthored material.

CURRICULUM VITAE

NAME OF AUTHOR: James Sartor

GRADUATE AND UNDERGRADUATE SCHOOLS ATTENDED:

University of Oregon, Eugene, OR, USA
University of La Sapienza, Rome, ITALY

DEGREES AWARDED:

Doctor of Philosophy, Physics, 2021, University of Oregon
Master of Science, Physics, 2017, University of La Sapienza
Bachelor of Science, Department of Physics, Physics, 2014, University of La Sapienza

AREAS OF SPECIAL INTEREST:

Soft Condensed Matter, Jamming, Rheology, Active Matter

PROFESSIONAL EXPERIENCE:

Research Assistant, University of Oregon, 2019-2021

Teaching Assistant, University of Oregon 2017-19

GRANTS, AWARDS AND HONORS:

Weiser Senior Teaching Assistant Award, UO Department of Physics, 2019

Weiser First Year Teaching Assistant Award, UO Department of Physics, 2018

PUBLICATIONS:

F. Arceri, E. I. Corwin, and Varda F. Hagh, "Marginal Stability Enables Memory Training in Jammed Solids" *arXiv preprint* arXiv:2106.05442 (2021)

F. Arceri, and E.I. Corwin, "Vibrational properties of hard and soft spheres are unified at jamming" *Phys Rev Letters* **112** (23) 238002 (2020).

F. Arceri, L. Berthier, G. Biroli, and F. Landes, "Glasses and aging: a statical mechanics perspective" *arXiv preprint* arXiv:2006.09725 (2020).

ACKNOWLEDGEMENTS

fill in this section This work was supported by the NSF Career Award grant No. DMR-1255370, and the Simons Collaboration on Cracking the Glass Problem (No. 454939 E. Corwin)

TABLE OF CONTENTS

LIST OF FIGURES

Figure Page

here is some text

CHAPTER I

DIRECT MEASUREMENT OF FORCE CONFIGURATIONAL ENTROPY IN JAMMING

Abstract

Thermal fluctuations are not large enough to lead to state changes in granular materials. However, in many cases, such materials do achieve reproducible bulk properties, suggesting that they are controlled by an underlying statistical mechanics analogous to thermodynamics. While themodynamic descriptions of granular materials have been explored, they have not yet been concretely connected to their underlying statistical mechanics. We make this connection concrete by providing a first principles derivation of the multiplicity and thus the entropy of the force networks in granular packings. We directly measure the multiplicity of force networks using a protocol based on the phase space volume of allowed force configurations. Analogous to Planck's constant, we find a scale factor, h_f, that discretizes this phase space volume into a multiplicity. To determine this scale factor, we measure angoricity over a wide range of pressures using the method of overlapping histograms and find that in the absence of a fundamental quantum scale it is set solely by the system size and dimensionality. This concretely links thermodynamic approaches of angoricity with the microscopic multiplicity of the force network ensemble.

Introduction

Thermodynamics connects abstract and difficult to measure details, such as entropy, with more easily measured bulk properties, such as temperature. In granular systems, for which the thermal energy scale is irrelevantly small, similar connections have been proposed for the volume ensemble [**? ?**] using compactivity as a temperature analog and also for the force network ensemble [**? ?**] using angoricity. While these quantities are measurable [**? ?**], they are not physically meaningful unless they 1) are shown to have temperature-like properties, such as following the zeroth law and 2) can be rigorously linked to a first principles definition of microscopic entropy [**?**]. Entropy itself was initially an empirical quantity until Sackur and Tetrode placed it on firm footing for the ideal gas with the discretization of phase space into quantum mechanical states [**? ?**]. The length scale of the discretization depends both on properties of the system and the universal constant $\hbar$, whose value cannot be inferred from bulk properties of the ideal gas alone. Angoricity holds promise as a temperature analog, as it has been shown to follow the zeroth law, while compactivity fails to do so [? ? ?]. However, before the thermodynamic approach of angoricity can be considered to be on solid ground, the nature of the entropy of jammed systems must first be understood.

When the density of an overjammed packing increases, force networks are affected in two ways: 1) force magnitudes, and thus pressure, increase, and 2) new contacts between particles form, increasing the number of contact forces in the network. Both of these changes increase the entropy of the force networks. While the effect on entropy from pressure changes is well understood [? ?], the effect from changes in the contact network is not. To decouple these effects, we propose an extension to the Force Network Ensemble in which changes in the contact network are allowed. This leads us to identify a critical number of excess contacts, δz_c, describing the transition from a regime in which entropy is dominated by changes in pressure to one in which it is dominated by changes in the contact network.

The temperature analogue angoricity is defined as the derivative of entropy with respect to the stress tensor [?]. In isotropic systems this tensor quantity can be simplified to a scalar derivative of entropy with respect to pressure. Just as temperature of an ideal gas can be measured from the velocity distribution, angoricity can be measured from the distribution of local pressures [?]. As a derivative, angoricity provides information about the difference in entropy between two systems but not the absolute values. Previous theoretical and experimental work has identified an inverse scaling of angoricity with pressure in the near jamming limit for two-dimensional (2D) soft spheres [? ?]. However, these studies do not systematically explore the effect of changing the contact network, which remains static in the near jamming limit. In our computational study, we explore the system by varying the spatial dimension, pressure, and number of particles over ranges much larger than would be feasible in a physical experiment.

In this Rapid Communication, we present a first principles derivation of the entropy for the force networks of granular packings. We measure this entropy up to a multiplicative constant, h_f, in the near jamming limit by directly measuring the volume of the space of allowed force configurations. Analogous to Planck's constant in the Sackur-Tetrode equation, h_f discretizes the space of force configurations into an integer number of accessible states. We then use the method of overlapping histograms to measure angoricity as a function of pressure, and compare with our

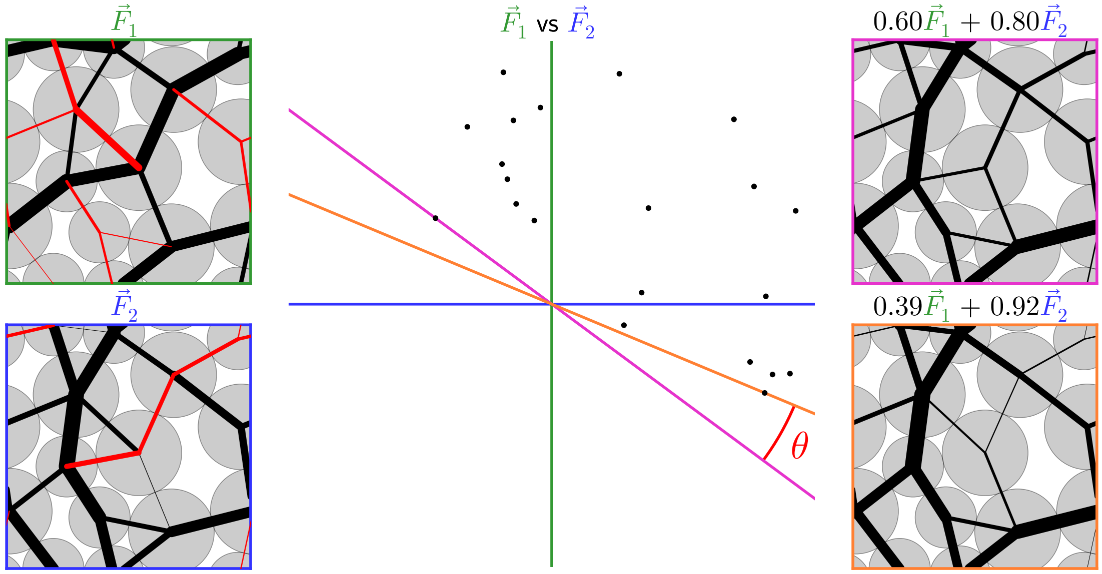

FIGURE 1. Force volume measurement for a system with one excess contact. Left, the two independent states of self stress, F_1 and F_2. Black lines between particles represent positive (compressive) forces, red lines represent negative (tensile) forces. Center, a scatter plot of F_1 vs F_2 for each pair of particles. Linear combinations of F_1 and F_2 are represented graphically by drawing a sloped line through the origin and measuring the distance to each point. Any sloped line for which all of the points fall into the same half-space corresponds to a positive definite linear combination. The set of lines which allow for such solutions is the force space volume, indicated by the angle θ. Note that in a system with ΔZ excess contacts, this volume is a ΔZ dimensional quantity. Right, the two extremal positive-definite linear combinations at the edge of this region are shown. Each has one force brought to precisely zero.

force volume measure to solve for h_f. This concretely connects the bulk nature of angoricity with the microscopic multiplicity of the force network ensemble.

Computational methods

We use pyCudaPacking [**?**], a GPU-based simulation engine, to generate energy minimized soft sphere packings at specified pressures in periodic boundary conditions. We do so for number of particles, N, spanning from 256 to 4096, and dimension, d, from 2 to 5. The particles are monodispersed, except in 2D in which we use equal numbers of bidispersed particles at a size ratio of 1.4:1 to prevent crystallization. Particles interact through a harmonic contact potential as defined in [**?**], and the system's energy is minimized using the FIRE minimization algorithm [**?**].

Starting with random initial positions, we minimize energy and then adjust overall density by uniformly scaling particle radii to achieve a pressure P of 10^{-2} in natural units, as defined in

[?]. This pressure is chosen to prevent crystallization artifacts from high density packings. From there, we iteratively adjust the density both up and down to achieve specific values of pressure. We do this efficiently by exploiting the known linear scaling of pressure with density above jamming for a harmonic potential [?]. For each targeted pressure, we ensure that the actual pressure is accurate to a factor of 10^{-5}. We sample 100 logarithmically spaced steps per decade of pressure to ensure sufficient overlap between the distributions of local pressure for neighboring systems, as is needed for the method of overlapping histograms.

Rigidity

To understand the behavior of packings close to the jamming transition we examine the geometric mechanisms necessary for rigidity by constructing an unstressed spring network with the geometry of the packing. The rigidity matrix [? ? ?], $\mathcal{R}$, describes this spring network by encoding the normalized contact force vectors from the packing, n_{ij}, between pairs of particles i and j as

$$\mathcal{R}^{k\alpha}_{\langle ij \rangle} = (\delta_{jk} - \delta_{ik}) n^{\alpha}_{ij}, \tag{1.1}$$

where k indexes contacts and α indexes spatial dimensions. For a system with N_{stable} stable particles and N_{contact} contacts, this will be an N_{contact} by $N_{\mathrm{stable}}d$ matrix. The singular value decomposition of this matrix yields two sets of singular vectors, analogous to eigenvectors for a square matrix. The right singular vectors describe the normal modes of position displacements, and the left singular vectors describe the normal modes of force displacements. The left singular vectors corresponding to zero eigenvalues represent mechanically stable force configurations, termed states of self stress. These vectors need not be positive definite, and therefore are not necessarily valid force configurations for the underlying packing.

The magnitude of each contact force can be considered as a degree of freedom while the requirement for mechanical stability introduces d constraints for each particle. Balancing these constraints requires a minimum number of contacts to ensure stability, which in systems with periodic boundary conditions is given by [? ?]

$$N^{\mathrm{min}}_{\mathrm{contact}} = d(N_{\mathrm{stable}} - 1) + 1. \tag{1.2}$$

A system with this minimum number of contacts has exactly one state of self stress, and each additional contact formed imparts an additional independent state of self stress. Thus, we define the number of excess contacts, ΔZ as

$$\Delta Z = N_{\text{contact}} - N_{\text{contact}}^{\text{min}}, \tag{1.3}$$

making the number of independent states of self stress $\Delta Z + 1$. We define the number of excess contacts per particle,

$$\delta z = 2\Delta Z/N, \tag{1.4}$$

where the 2 reflects that each excess contact is shared between two particles. These independent states of self stress form a basis for the $\Delta Z + 1$ dimensional space of all mechanically stable force configurations of the spring network. However, imposing a normalization condition restricts this to a ΔZ dimensional subspace.

Force Volume

The force network ensemble samples all valid force networks in the spring representation of a packing with equal probability [**? ? ?**]. To determine the force volume, we calculate the normalized independent states of self stress where F_μ^q is the contact force on contact q in the state of self stress μ. The set of all possible repulsive contact forces is defined by linear combinations that satisfy

$$\sum_\mu \lambda_\mu F_\mu^q \geq 0 \tag{1.5}$$

for all contacts q, where $\{\lambda_\mu\}$ are coefficients subject to the normalization condition $\sum_\mu \lambda_\mu^2 = 1$. We define the force volume V_f to be the volume of the space of λ_μ coefficients that satisfy this rule as illustrated in Fig. 1.

We measure this force volume with the following protocol:

1. Recast F_μ^q into a set, $\{\vec{C}^q\}$, of N_{contacts} vectors containing the value of the force on contact q in each of the $\Delta Z + 1$ states of self stress.

2. Planes which pass through the origin and place all of the $\{\vec{C}^q\}$ into a single half-space satisfy inequality (1.5). We compute the extremal values of such planes as the facets of the convex hull [**?**] of $\{\vec{C}^q, \vec{0}\}$. The normal vector to each facet is the $\{\lambda_\mu\}$ which defines a vertex of the allowed space of coefficients and corresponds to a linear combination of the independent states of self stress in which exactly ΔZ forces are precisely 0.

3. To respect the normalization requirement we calculate V_f as the ΔZ dimensional solid angle subtended by the volume defined by these vertices in coefficient space.

We convert this volume into a pure number of configurations by discretizing it into hypercubes of side length h_f, named to emphasize the parallelism with Planck's constant h used in the enumeration of phase space states in the Sackur-Tetrode equation. Because the pressure sets the scale of the average force, we then multiply this enumeration by the pressure, as has been shown in previous theoretical and experimental work [**? ? ?**]. Putting these considerations together, we arrive at an ansatz relating the microscopic force volume to the multiplicity, and thus the entropy:

$$\Omega = P\frac{V_f}{(h_f)^{\Delta Z}} \qquad \Longrightarrow \qquad S = \ln P + \ln V_f - \Delta Z \ln h_f. \tag{1.6}$$

Although pressure and number of excess contacts both appear in the entropy, they are not independent variables but related in the thermodynamic limit by [**? ?**]

$$\Delta Z = B(d)N\sqrt{P}. \tag{1.7}$$

where B is some function of dimension only. We find values of B of approximately 2.1, 6.0, 12.5, and 23 in dimensions two, three, four, and five. These values are roughly consistent with previous studies for two and three dimensional spheres [**? ?**].

Angoricity [**?**], α, is derived as:

$$\alpha \equiv \frac{\partial S}{\partial P} = \frac{1}{P} + \frac{\partial}{\partial P}\ln V_f - \frac{1}{2}\frac{BN}{\sqrt{P}}\ln h_f. \tag{1.8}$$

First, we measure the volume of force space V_f and explore how it scales with the number of excess contacts. Second, we measure bulk angoricity to confirm our prediction in Eq. (1.8) and measure the microscopic constant h_f.

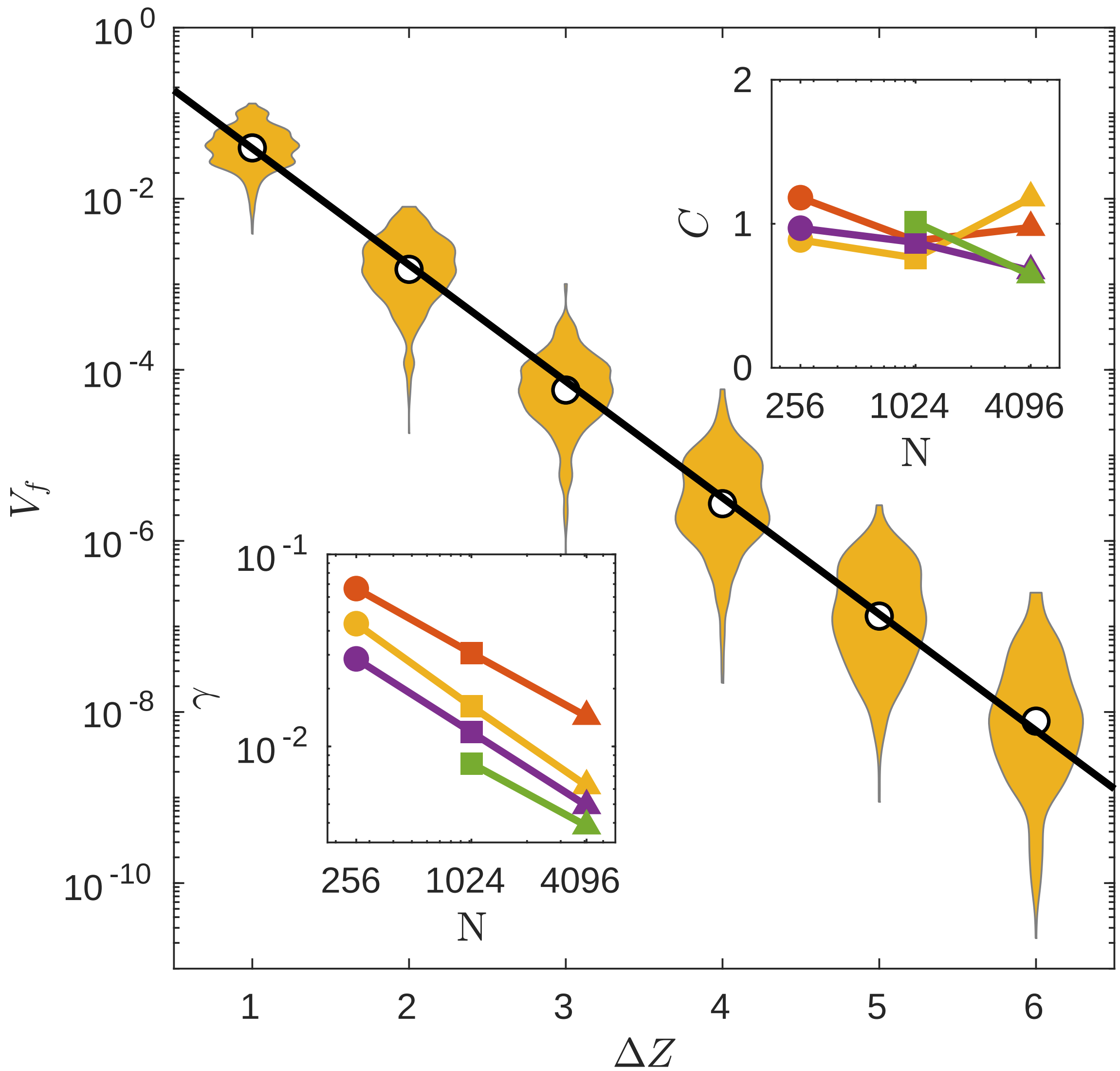

FIGURE 2. Representative exponential scaling of the force volume, V_f, with number of excess contacts, ΔZ, for $N = 1024$, $d = 3$. The median of the distribution for each ΔZ is shown as a white circle, surrounded by the full distribution in yellow. The black line shows the exponential fitting form, with exponential base γ. Inset bottom left, γ for each N and d. Inset top right, the scale, C of the exponential. Inset data is presented for $d = 2$ (red), 3 (yellow), 4 (purple), and 5 (green), and $N = 256$ (circles), 1024 (squares), and 4096 (triangles).

Results

As shown in Fig. 2, the measured force volume scales exponentially with the number of excess contacts:

$$V_f \;=\; C\gamma^{\Delta Z}. \tag{1.9}$$

We find C to be well approximated by 1, as shown in the top inset. The lower inset shows that γ decreases with increasing N and d.

We can simplify the expression for angoricity by combining the preceding three equations to find

$$\alpha = \frac{1}{P} + \frac{1}{\sqrt{P_c P}} \tag{1.10}$$

where the crossover pressure between the two power laws is

$$P_c = \left[\frac{BN}{2}\ln\left(\frac{\gamma}{h_f}\right)\right]^{-2}. \tag{1.11}$$

We use the method of overlapping histograms of local pressures [**?** **?** **?**] to measure angoricity and determine the value of P_c and therefore h_f. For each system, we measure the local pressure for many random samples of a particle with its $m = 50$ nearest neighbors. The choice of m controls the sharpness of the local pressure distribution and so induces a trivial prefactor A, shown in the inset to Fig. 3 to be proportional to dm. We then compute the angoricity by comparing these local pressure distributions as in Ref [**?**]. We fit the angoricity curve to the power law in Eq. (1.10) with prefactor A and an additive offset. As shown in Fig. 3, all data collapse onto Eq. (1.10). We extract the crossover pressures, P_c, shown in the upper inset of figure 3, and find that they are insensitive to N, but decrease with increasing d.

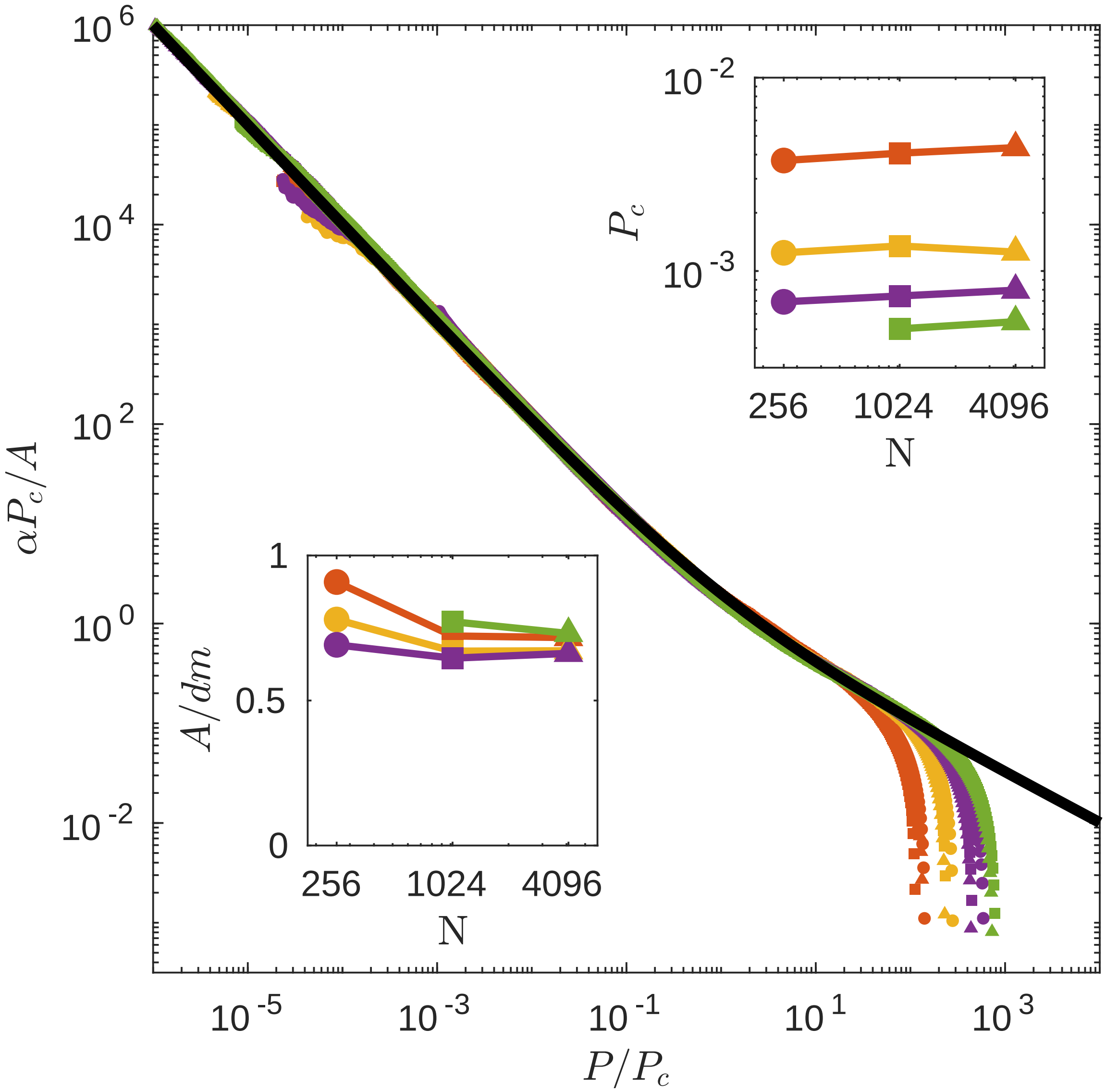

FIGURE 3. Scaled angoricity, $\alpha P_c/A$, for all N and d, collapses onto equation 1.8 (black line) when plotted against scaled pressure, P/P_c, until high pressure deviations caused by second nearest neighbor interactions. Inset top right, the crossover pressure P_c. Inset bottom left, A/dm is approximately 0.7. Colors denote dimension from 2-5 and symbol denotes number of particles as in figure 2.

Discussion

From Eq. (1.11) and our measured values of γ and P_c we compute h_f, shown in the inset to Fig. 4. A complete expression for entropy can now be written as

$$S = \ln P + \Delta Z \ln \left(\frac{\gamma}{h_f} \right). \tag{1.12}$$

This can be recast into a natural form using equations (1.7) and (1.10) by expressing the ratio of γ and h_f as a critical number of excess contacts per particle,

$$\delta z_c = 2B\sqrt{P_c} = \frac{2}{N \ln\left(\frac{\gamma}{h_f}\right)} \tag{1.13}$$

$$S = \ln P + \frac{\delta z}{\delta z_c}. \tag{1.14}$$

Thus, the entropy is dependent on two intensive thermodynamic variables, P and δz, and a constant δz_c for each dimension. While h_f is observed to decrease with N and expected to vanish in the thermodynamic limit, we find δz_c to be intensive with system size, as shown in Fig. 4.

The first term in Eq. (1.14) describes the entropy increasing from the absolute pressure scale, whereas the second describes the entropy increasing from the number of contacts increasing. Sufficiently close to jamming the first term will dominate as there will be few changes in the contact network even as the pressure changes dramatically. Further from jamming the second term will dominate, reflecting the primacy of changes in the contact network. Note that while this equation may be rewritten as a function of pressure using Eq. (1.7), for any particular finite packing the integer number of excess contacts is required to calculate the entropy precisely.

Conclusion

We have demonstrated that the force network ensemble framework can be used to directly compute the multiplicity of the force configurations in packings close to the critical jamming point. We have presented an ansatz linking the volume of the force configurational space associated with a packing to the entropy of the packing. This entropy can be expressed as a function of pressure and is independently confirmed by measurements of the angoricity over approximately seven orders of magnitude of pressure. We have combined these two approaches of measuring entropy in order to extract the fundamental scales governing the discretization of phase space that allows for enumeration. We discover a crossover value for the excess contacts per particle, δz_c, below which the entropy is governed primarily by changes in pressure at fixed contact network and above which the entropy is governed primarily by the creation of new contact forces.

This work places angoricity on a firm footing as a thermodynamic quantity that controls the behavior of overjammed systems. By tracing this entropy all the way down to an enumeration of states we discover that, perhaps unsurprisingly, Planck's constant does not set the fundamental scale of discretization h_f. In a purely classical model such as this, the discretization can only depend on the finite size effects of the system which are determined by N and d. Thus, in the thermodynamic limit, while h_f vanishes, the behavoir of the system is controlled by δz_c and thus P_c which do obtain fixed values. This full expression for entropy provides the first concrete linking of the microscopic force network ensemble to the thermodynamic description of granular materials and offers a complete description for the thermodynamics of the force networks in overjammed systems.

Acknowledgments

We thank Bulbul Chakraborty, Karen Daniels, Sean Ridout, and Brian Tighe for useful discussions. This work benefited from access to the University of Oregon high performance computer, Talapas. This work was supported by National Science Foundation (NSF) Career Award DMR-1255370 and the Simons Foundation Grant No. 454939.

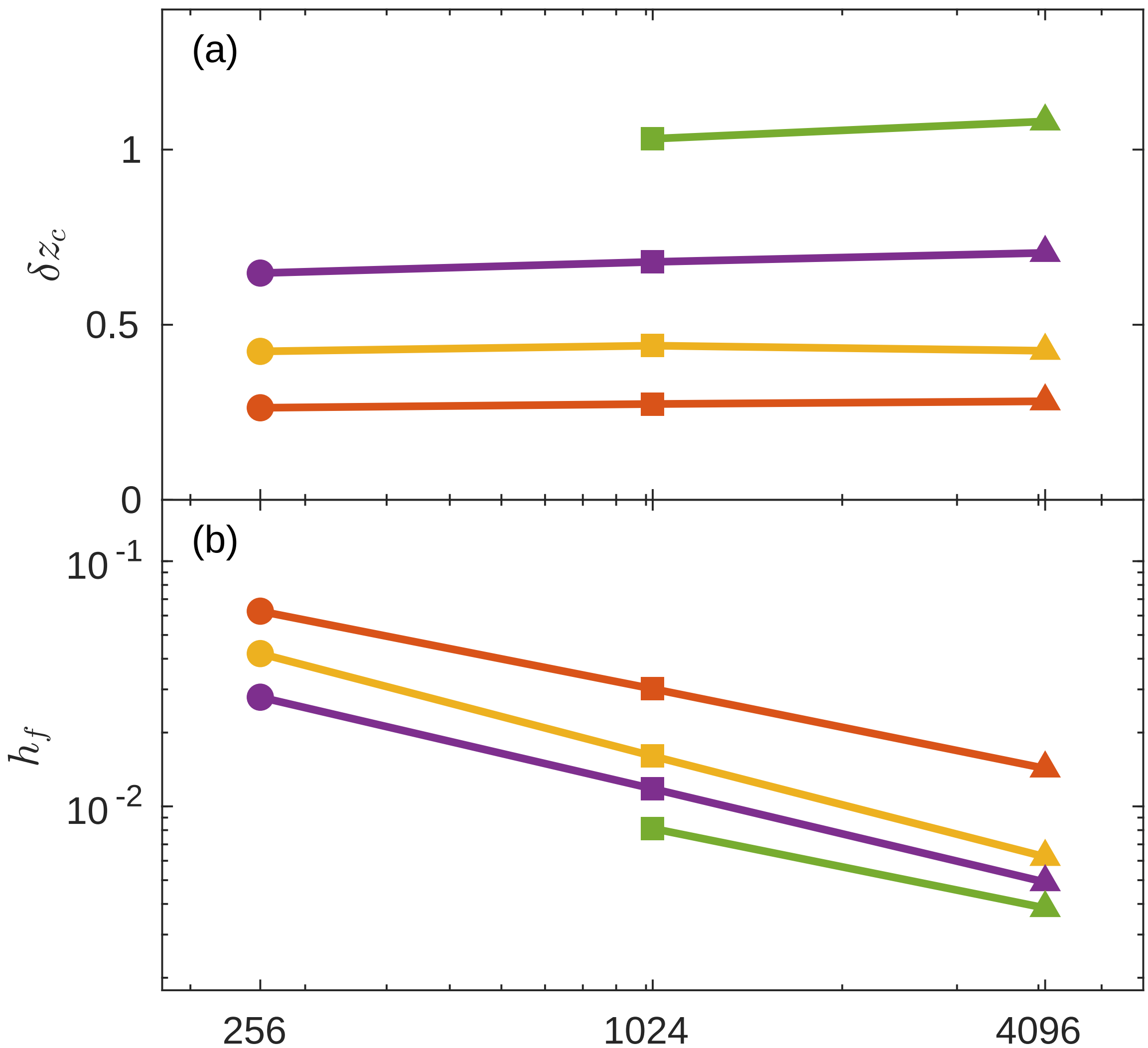

FIGURE 4. Upper, scaling of δz_c with N and d. Lower, scaling of h_f, with N and d, calculated from P_c by inverting equation 1.11. Colors denote dimension from 2-5 and symbol denotes number of particles as in figure 2.

CHAPTER II

MEAN-FIELD PREDICTIONS OF SCALING PREFACTORS MATCH LOW-DIMENSIONAL JAMMED PACKINGS

No known analytic framework precisely explains all the phenomena observed in jamming. The replica theory for glasses and jamming is a mean-field theory which attempts to do so by working in the limit of infinite dimensions, such that correlations between neighbors are negligible. As such, results from this mean-field theory are not guaranteed to be observed in finite dimensions. However, many results in mean field for jamming have been shown to be exact or nearly exact in low dimensions. This suggests that the infinite dimensional limit is not necessary to obtain these results. In this Letter, we perform precision measurements of jamming scaling relationships between pressure, excess packing fraction, and number of excess contacts from dimensions 2–10 in order to extract the prefactors to these scalings. While these prefactors should be highly sensitive to finite dimensional corrections, we find the mean-field predictions for these prefactors to be exact in low dimensions. Thus the mean-field approximation is not necessary for deriving these prefactors. We present an exact, first-principles derivation for one, leaving the other as an open question. Our results suggest that mean-field theories of critical phenomena may compute more for $d \geq d_u$ than has been previously appreciated.

Introduction

Granular materials exhibit universal properties regardless of the material properties of the individual grains [**? ? ?**]. The jamming transition is a critical point near which properties such as pressure, packing fraction, or number of excess contacts, among others, scale as power laws. Scaling theory summarizes and condenses these power law relationships, but no first-principles theory of jammed systems at finite dimensions exists. The replica mean-field theory of glasses and jamming has been shown to be exact in the infinite dimensional limit [**? ?**]. To do so it relies on the assumption that there are no correlations between neighbors, fundamentally at odds with low-dimensional systems. As such, mean-field predictions should not be expected to hold in low dimensional-jamming, and some results, most notably the packing fraction at jamming, deviate from the mean-field predictions [**? ?**]. However, despite the fact that low dimensional systems have highly correlated neighbors the scaling relations are precisely the same as those found in infinite dimensions [**? ? ?**]. Many other results predicted by the mean field have also been observed in low dimensional jamming, suggesting that they may be provable without the mean field approximation [**? ? ? ? ? ?**].

Here, we move one step further in the comparison between low-dimensional jamming and mean-field jamming by probing not only scaling relations but also prefactors between a handful of properties: pressure P, excess contacts δz, and excess packing fraction above jamming $\Delta\varphi$. We demonstrate the continued success of the mean field in describing low-dimensional systems by quantitatively verifying the mean-field predictions for these prefactors. Thus, the mean-field approximation is overzealous: one need not have vanishing correlations in order to obtain these results. In this spirit we provide a first-principles proof of the relation between pressure and excess packing fraction free of the mean-field assumptions. These results call out for proofs for all of the other universal relations of the jamming transition.

Background

Granular materials undergo a jamming transition at a critical packing fraction φ_j. The number of force bearing contacts between grains jumps abruptly from zero to the minimum number sufficient to support global rigidity and thus global pressure, Z_c. In a packing of N frictionless, spherical particles in d dimensions, $Z_c = Nd + 1 - d$ [**? ?**].

We limit our study to spherical particles interacting through a harmonic contact potential given by

$$U_{ij} = \varepsilon \left(1 - \frac{|\mathbf{r}_{ij}|}{\sigma_{ij}}\right)^2 \Theta\left(1 - \frac{|\mathbf{r}_{ij}|}{\sigma_{ij}}\right), \tag{2.1}$$

where ε is the energy scale, $\mathbf{r_{ij}}$ is the contact vector between particles i and j, σ_{ij} is the sum of the radii of particles i and j, and Θ is the Heaviside step function. Thus, the total energy $U = \frac{1}{2}\sum_{ij} U_{ij}$. From this potential, the forces between particles can be calculated as

$$\mathbf{f}_{ij} = \frac{2\varepsilon}{\sigma_{ij}} \left(1 - \frac{|\mathbf{r_{ij}}|}{\sigma_{ij}}\right) \Theta\left(1 - \frac{|\mathbf{r_{ij}}|}{\sigma_{ij}}\right) \hat{r}_{ij}. \tag{2.2}$$

We compute a unit and dimension independent pressure using the microscopic formula [**? ?**]

$$P \equiv -\frac{\bar{V}_p}{\varepsilon}\frac{dU}{dV} = \frac{\bar{V}_p}{\varepsilon V d}\sum_{i,j}\mathbf{f}_{ij}\cdot\mathbf{r}_{ij}, \tag{2.3}$$

where V is the volume of the system and $\bar{V}_p$ is the average particle volume.

For soft spheres the packing fraction φ can be increased, leading to new contacts and an increased pressure. We thus consider three natural quantities that measure distance from jamming:

– excess packing fraction, $\Delta\varphi = \varphi - \varphi_j$

– excess contacts per particle, $\delta z = (Z - Z_c)/N$ where Z is the number of contacts

– pressure P

The relationships between these quantities are predicted by mean-field theory as [**?**]:

$$P = C_{p\varphi}\Delta\varphi \tag{2.4}$$

$$\delta z = C_{zp}P^{1/2} \tag{2.5}$$

with prefactors $C_{p\varphi}$ and C_{zp} which are functions only of spatial dimension [**?**]. These and other scaling relationships have been previously explained by approximate theories [**? ? ? ?**] and computationally confirmed in low-dimensional jamming [**? ? ? ?**]. They are summarized concisely by the scaling theory of the jamming transition [**?**]. The scaling exponents in $d \geq 2$ match those in mean field, suggesting that the transition behaves like a critical point with upper critical dimension $d_u = 2$. Moreover, mean-field theory predictions of these prefactors can be derived as [**? ?**]:

$$C_{p\varphi} = \frac{1}{d}\hat{C}_{p\varphi} \tag{2.6}$$

$$C_{zp} = \frac{d}{\sqrt{2^d}}\hat{C}_{zp} \tag{2.7}$$

where $\hat{C}_{p\varphi}$ and $\hat{C}_{zp}$ are finite constants in the $d \to \infty$ limit, which have not yet been explicitly calculated. Note that these relations are presented in a particular choice of units in the literature. We include details of the conversion to our dimensionless units in the Supplemental Material. *A* *priori*, it is not expected that these predictions will apply in low dimensions, in which the mean-field assumption is not warranted. Even above upper critical dimensions, mean-field theories are not generally expected to correctly compute prefactors, or even the purportedly universal amplitude ratios. Beyond scaling exponents, to our knowledge, the critical cluster shape in percolation and related phenomena [**?** **?**] and the Binder cumulant in the Ising model [**?** **?** **?**] are the only quantities which are known to be equal to their mean-field values above the upper critical dimension. Even though these prefactors for jamming scaling relationships have been measured and reported [**?** **?**], because they are not expected to be equal to their mean-field values they have not received substantial theoretical attention. An approximate calculation of the related prefactor between the shear modulus and number of excess contacts has been performed in three dimensions [**?**].

Computational methods

We use pyCudaPacking [**?**], a GPU-based simulation engine, to generate energy minimized soft (or penetrable) sphere packings. We do so for number of particles $N = 8192 - 32768$ and dimension $d = 2 - 10$. Our results suggest that $N = 8192$ is large enough to avoid finite size effects in $d < 9$, which we have verified in $d = 8$ by comparing our packing at $N = 8192$ with one at $N = 16384$, finding no deviation. For $d = 9$ and $d = 10$ we use system sizes of 16384 and 32768, respectively. The particles are monodisperse, except in two dimensions in which we use equal numbers of bidisperse particles with a size ratio of 1:1.4 to prevent crystallization.

The packings are subject to periodic boundary conditions. We minimize the packings using the FIRE minimization algorithm [**?**] using quad precision floating point numbers in order to achieve resolution on the contact network near the jamming point.

Using the same methods as described in Ref. [**?**], we start with randomly distributed initial positions, and apply a search algorithm to create systems approximately logarithmically spaced in $\Delta\varphi$. At each step we use the known power law relationship between energy and $\Delta\varphi$ to calculate an estimate of φ_j. We use this estimate to approximate $\Delta\varphi$ and determine the next value of φ in an effort to logarithmically space $\Delta\varphi$ values. We then adjust the packing fraction to this value of φ by uniformly scaling particle radii and minimizing the system. We continue this process until the system is nearly critically jammed, i.e. has exactly one state of self stress.

We then use the known power law relationship between pressure and $\Delta\varphi$ to fit the dataset and precisely calculate φ_j (with error less than the smallest value of $\Delta\varphi$) from which we calculate $\Delta\varphi$ at each value of φ.

Results

Figure 5 shows the measured linear scaling of pressure with packing fraction separately for each dimension. We fit the data to Eq. 2.4 to find $C_{p\varphi}$, considering only data close to jamming to avoid fitting to high pressure deviations from the scaling power law. The measured values of $C_{p\varphi}$ are shown in the inset to confirm the $1/d$ dimensional scaling predicted by mean-field theory in Eq. 2.6. A fit to this scaling provides a value of $\hat{C}_{p\varphi}$ of 1.23.

Figure 6 shows the measured square root scaling of excess contacts with pressure separately for each dimension. We fit the data to Eq. 2.5 to find C_{zp}, the values of which are shown in the inset. Beginning around three dimensions, the values of C_{zp} confirm the dimensional scaling predicted by mean-field theory in Eq. 2.7, and a fit to this scaling provides a value of $\hat{C}_{zp}$ of 0.74.

The values of both $C_{p\varphi}$ and C_{zp} are roughly consistent with values measured in previous studies [**?** **?**]. It has been recently suggested that the prestress, i.e., the normalized ratio of the first and second derivatives of the potential as defined in Ref. [**?**], is a better candidate to dedimensionalize the relationship between pressure and excess contacts. However, we find a substantially better collapse of our expected form of pressure than with prestress. For more details on prestress, see the attached Supplemental Material.

Discussion

The close agreement of our data with the mean-field predictions in low dimensions suggests that the mean-field assumption is not essential to derive these scaling and prefactor relations. In the spirit of discovering proofs for these relations free of the mean-field assumption, we expand on an earlier calculation of the bulk modulus scaling [**?**] to show that such a calculation can also explain the scaling of $C_{p\varphi}$ with spatial dimension and the precise value of $\hat{C}_{p\varphi}$.

From taking a derivative of Eq. 2.4, we see immediately that $C_{p\varphi}$ may be expressed in terms of the bulk modulus, $K \equiv V \frac{d^2U}{dV^2}$, at jamming:

$$C_{p\varphi} = \frac{\bar{V}_{\mathrm{p}} V}{\varphi \varepsilon} \frac{d^2U}{dV^2} = \frac{V}{N\varepsilon} K. \tag{2.8}$$

We note that this approximation slightly overestimates $C_{p\varphi}$: the apparently linear average stress-strain curves of jammed packings are actually the average of many piecewise linear curves with discontinuous drops in stress, thus the average slope is slightly less than the instantaneous slope [**?**].

At the unjamming point, the linear response of the system is that of a network of unstretched springs. Thus, at lowest order in pressure the bulk modulus is that of an unstressed spring network, which may be calculated in terms of the "states of self stress," vectors of possible spring tensions, $s \in \mathbb{R}^Z$, which do not produce any net force on a particle [**? ? ?**]. Here we explain how to carry out this calculation for a monodisperse system in the unjamming limit; a correction for polydispersity is handled in the Supplemental Material.

We begin by defining the set of "affine bond extensions," a vector $E \in \mathbb{R}^Z$ giving the amount by which each bond vector would increase under a unit volumetric expansion of the system. In linear elasticity, this simply induces an expansion of each length by $1/d$, so,

$$E_\ell = \frac{1}{d} r_\ell, \tag{2.9}$$

where we emphasize that ℓ indexes the contacts in the system rather than the particles; r_ℓ is the distance between a particular pair of particles.

In the case that all springs have the same spring constant k (e.g., monodisperse packings), the bulk modulus may be written as the projection of these affine moduli onto the states of self stress [**? ? ?**]. At jamming, there is only one state of self stress, and so the bulk modulus may be computed exactly using the projection onto only this one state of self stress [**?**],

$$K = \frac{k}{V} \left(\sum_{\ell=1}^{Z} s_{1,\ell} E_\ell \right)^2 \tag{2.10}$$

$$= \frac{2N\varepsilon}{dV} \frac{\langle f \rangle^2}{\langle f^2 \rangle} \tag{2.11}$$

In the near jamming limit, this one special state of self stress exists all the way down to the jamming point and can be expressed in terms of the vector of physical force magnitudes, f. For the packing to be in equilibrium, this set of contact forces must produce no net force on every particle, and thus by definition the vector f is always a state of self stress. The projection defined above requires states of self stress to be normalized, and so the state of self stress may be expressed as:

$$s_{1,\ell} = \frac{1}{\sqrt{\sum_l f_l}} f_\ell = \frac{1}{\sqrt{Z\langle f^2 \rangle}} f_\ell. \tag{2.12}$$

Furthermore at lowest order in P we have $r = \sigma$, and we assume $Z \approx dN$. Thus, Eq. 2.10 reduces to

$$K = \frac{Nk\sigma^2}{dV} \frac{\langle f \rangle^2}{\langle f^2 \rangle} = \frac{2N\varepsilon}{dV} \frac{\langle f \rangle^2}{\langle f^2 \rangle} \tag{2.13}$$

and thus via Eq. 2.8

$$C_{p\varphi} = \frac{2}{d} \frac{\langle f \rangle^2}{\langle f^2 \rangle}, \tag{2.14}$$

for monodisperse spheres. The full calculation in the Supplemental Material shows that in the polydisperse case this becomes

$$C_{p\varphi} = \frac{2}{d} \frac{\langle \sigma f \rangle^2}{\langle \sigma^2 f^2 \rangle}. \tag{2.15}$$

We find that the distribution of contact forces does not depend strongly on dimension, which we demonstrate and discuss in the Supplementary Material, including Refs. [**?** **?**]. We thus predict the scaling of $C_{p\varphi}$ to agree with the asymptotic mean-field scaling. Because this proof does not invoke the mean-field assumption, we expect this scaling to be correct in all dimensions. Moreover, we are able to calculate each value of $C_{p\varphi}$ by measuring the ratio of force distribution moments. These values are calculated as in Eq. 2.15, and are shown in Fig. 5 to precisely predict the values of $C_{p\varphi}$.

Conclusion

The mean-field theory of jamming predicts both the scaling exponents and the dimensional scaling of their prefactors. While the exponents have been previously verified, we have demonstrated that even some prefactors are well predicted in low dimensions by mean-field theory. Although these prefactors should be considered especially sensitive to finite dimensional corrections, we find the mean field prediction to be exact in low dimensions. Is this a generic phenomenon, or are the quantities we have chosen to study in this work somehow specially unaffected by finite dimensional correlations? Experience with critical phenomena suggests that although certain ratios of these prefactors (i.e. amplitude ratios) may be universal, the prefactors themselves should be both nonuniversal and challenging to compute, which has led to them being neglected. Our results demonstrate however that these prefactors may be computed exactly. These results call out for other theories of jamming and the glass transition which reproduce the mean-field results without such assumptions, or perhaps for a deeper understanding of why certain mean-field computations may be exact in finite dimensions. Additionally, our results suggest that in traditional critical phenomena mean-field theory may compute more for $d \geq d_u$ than has been previously appreciated.

Acknowledgments

We thank Francesco Zamponi for generous assistance in interpreting the mean-field results. We also thank Andrea Liu, Jim Sethna, Cam Dennis, and Aileen Carroll-Godfrey for valuable discussion and feedback. This work benefited from access to the University of Oregon high performance computer, Talapas. This work was supported by National Science Foundation (NSF) Career Grant No. DMR-1255370 and the Simons Foundation No. 454939 (J.D.S. and E.I.C.) and by an NSERC PGS-D fellowship and Simons Foundation No. 454945 to Andrea J. Liu. (S.A.R.).

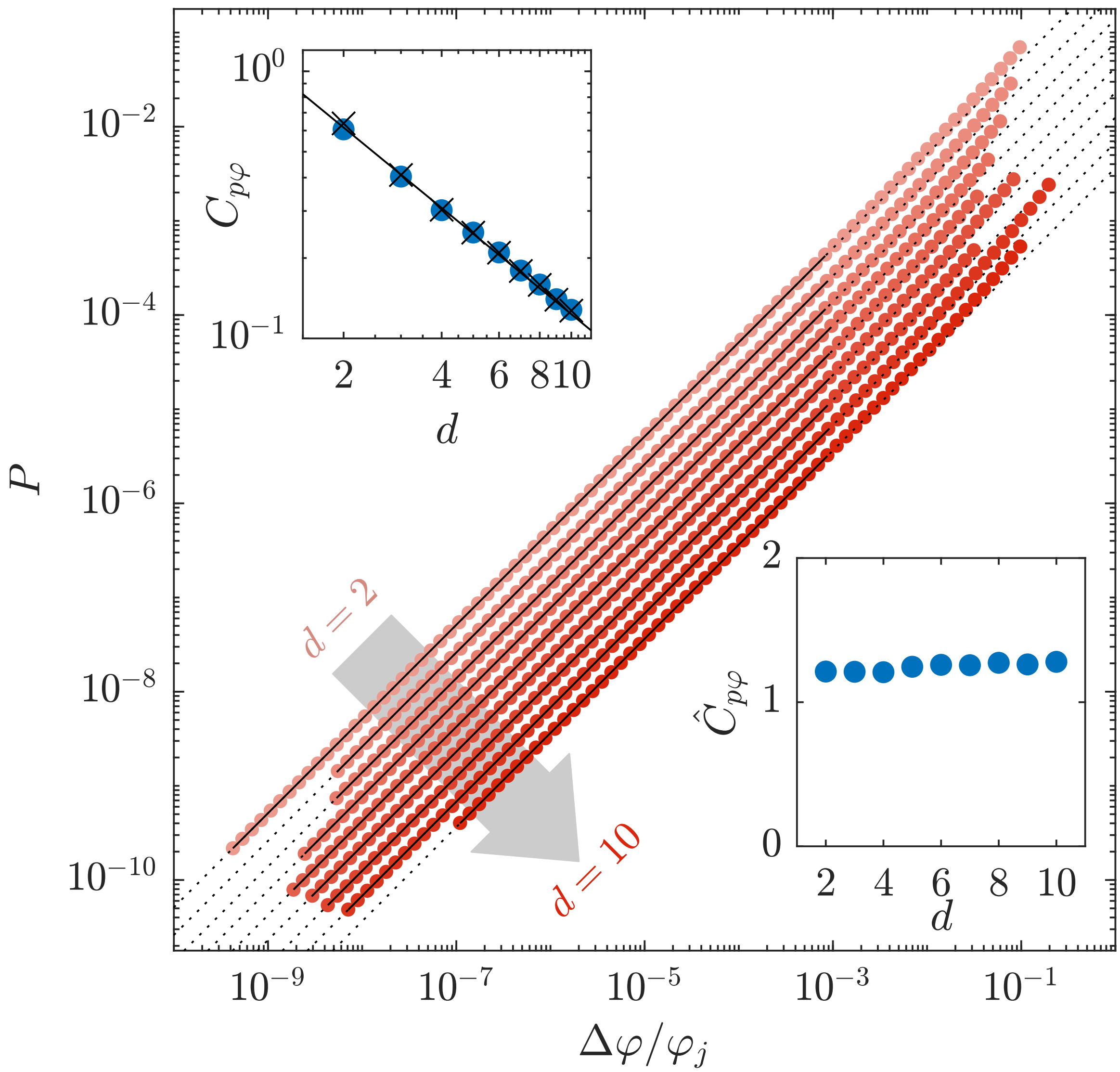

FIGURE 5. Measured pressure scales linearly with scaled excess packing fraction for systems from $d = 2$ to $d = 10$. Measured values for φ_j in our protocol are included in the Supplemental Material. Black lines show fits for $C_{p\varphi}$ using Eq. 2.4. We exclude from the fit data with $\Delta\varphi/\varphi_j > 10^{-3}$, to avoid the effect of larger overlaps causing deviations from this power law. Dotted lines show the extension of fits beyond fitted range. Upper inset shows the measured values of $C_{p\varphi}$ (blue circles) to scale in agreement with the mean-field prediction Eq. 2.6, shown as a fit to a black line with $\hat{C}_{p\varphi} \approx 1.23$. Moreover, they are in precise agreement with predicted values from Eq. 2.15 (marked with black $\times$'s). Lower inset shows measured values of $\hat{C}_{p\varphi}$ calculated from the measured values of $C_{p\varphi}$ and eqn 2.6. While each prefactor is measured from a single system, the prefactors for a second, identically constructed dataset were calculated to be well within the bounds of the marker size.

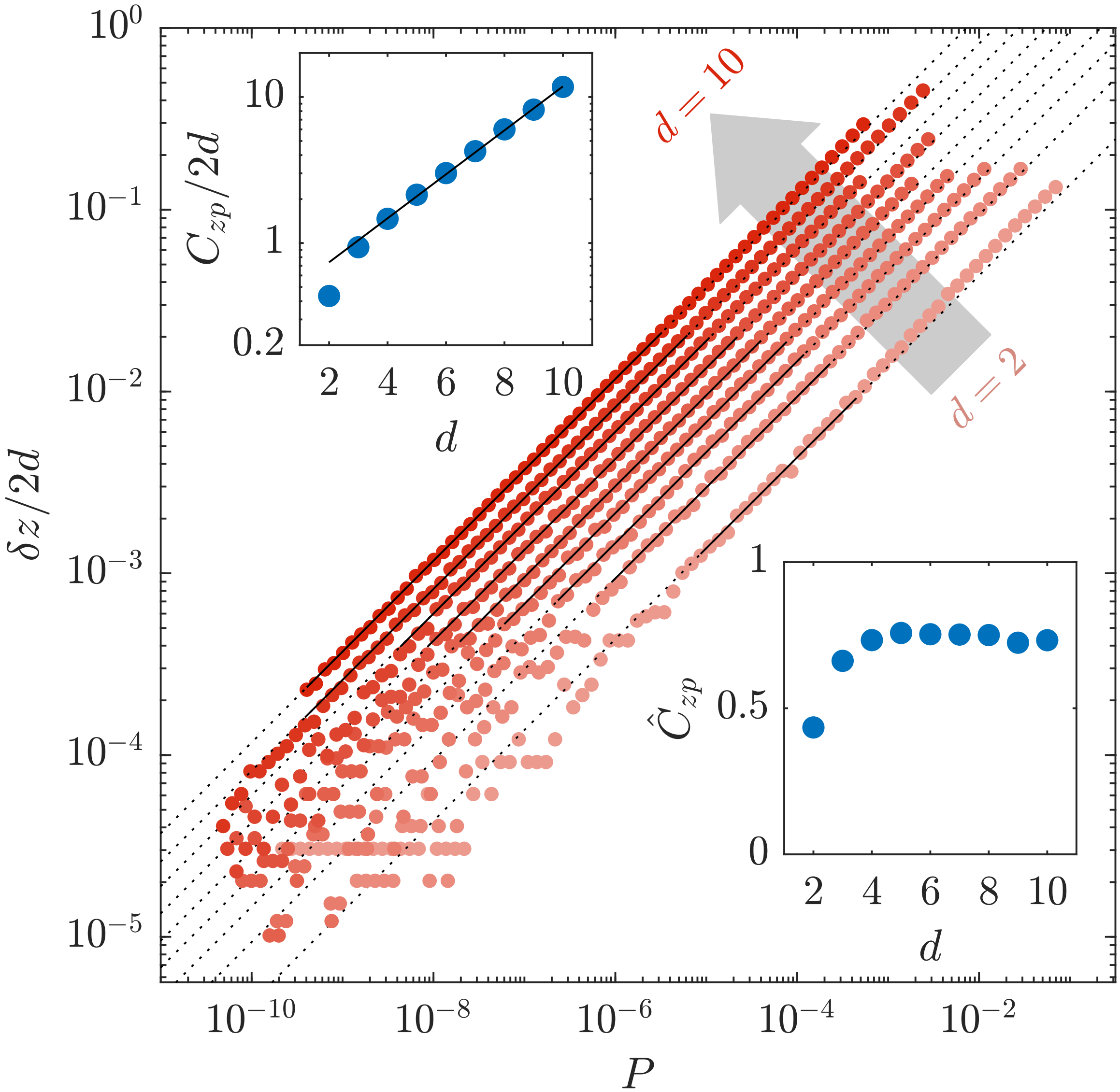

FIGURE 6. Measured excess contacts scales with the square root of pressure for systems from $d = 2$ to $d = 10$. Black lines show fits for C_{zp} using Eq. 2.5. For our fits, we ignore high pressure data as in Fig. 5, and additionally exclude data with less than 40 excess contacts to avoid fitting to small number fluctuations. Dotted lines show the extension of our fits beyond fitted range. Lower inset shows the measured values of C_{zp} (blue circles), which scale in agreement with the mean-field prediction Eq. 2.7, shown as a fit to a black line and with $\hat{C}_{zp} \approx 0.74$. Upper inset shows measured values of $\hat{C}_{zp}$ calculated from the measured values of C_{zp} and Eq. 2.7. While each prefactor is measured from a single system, the prefactors for a second, identically constructed dataset were calculated to be well within the bounds of the marker size.

CHAPTER III

SUPPLEMENTARY MATERIAL OF "MEAN-FIELD PREDICTIONS OF SCALING PREFACTORS MATCH LOW-DIMENSIONAL JAMMED PACKINGS"

Measured values of φ_j

In Table 1 we show our measued values of φ_j. these values are used in calculating $\Delta\varphi$.

TABLE 1. Measured values of φ_j in dimensions 2-10.

d	2	3	4	5	6	7	8	9	10
φ_j	0.85	0.65	0.46	0.31	0.20	0.13	0.078	0.049	0.029

Mean Field Predictions of Prefactors

Mean Field Prediction of Pressure vs Packing Fraction

Mean field theory predicts that pressure scales with packing fraction as follows [**?**]:

$$\hat{P} = \hat{C}(\hat{\varphi} - \hat{\varphi}_j) \tag{3.1}$$

where $\hat{C}_{p\varphi}$ is a constant, and the hats over P and $\Delta\varphi$ signify that the quantities are scaled such to be fixed in the infinite dimensional limit, as follows:

$$\hat{P} = \frac{P^*}{\rho d} \tag{3.2}$$

$$\hat{\varphi} = \frac{2^d}{d}\varphi \tag{3.3}$$

where ρ is the number density, $\frac{N}{V}$, and P^* is the pressure which is calculated with assumed unit particle diameter. This relates to our pressure, P, as follows:

$$P = \frac{\varphi}{\rho}\frac{1}{d^2}P^*, \tag{3.4}$$

where the factor of $\frac{\varphi}{\rho}$ unwraps their assumption of unit particle diameter, and the factor of $\frac{1}{d^2}$ comes from their potential, which explicitly contains a dimensional term:

$$U^*(r) = \frac{\epsilon d^2}{2}\left(\frac{r}{\ell} - 1\right)^2 \Theta\left(\ell - r\right). \tag{3.5}$$

We can thus rewrite equation 3.2 in terms of our pressure P:

$$\hat{P} = \frac{d}{\varphi}P, \tag{3.6}$$

and therefore equation 3.1:

$$\frac{d}{\varphi}P = \hat{C}\frac{2^d}{d}(\varphi - \varphi_j) \tag{3.7}$$

$$P = \frac{\varphi}{d}\hat{C}\frac{2^d}{d}\Delta\varphi \tag{3.8}$$

$$P = \frac{1}{d}\hat{C}\hat{\varphi}_j(\Delta\varphi) \tag{3.9}$$

$$P = \frac{1}{d}\hat{C}_{p\varphi}(\Delta\varphi). \tag{3.10}$$

Where, noting that $\hat{\varphi}_j$ and $\hat{C}$ are constants in the infinite dimensional limit, we combine them as $\hat{C}_{p\varphi}$. Thus mean field predicts a simple $1/d$ scaling of the prefactor between pressure and excess packing fraction.

Mean Field Prediction of Pressure vs Number Of Excess Contacts

The number of contacts, z, is predicted by mean field theory to have the form [**?**]:

$$\frac{z}{2d} = 1 + \hat{C}_{z\varphi}\sqrt{\hat{\varphi} - \hat{\varphi}_j} \tag{3.11}$$

$$\frac{z}{2d} = 1 + \hat{C}_{z\varphi}\sqrt{\frac{2^d}{d}}\sqrt{\varphi - \varphi_j} \tag{3.12}$$

for some constant $\hat{C}_{z\varphi}$.

The number of excess contacts, δz, therefore is predicted to scale as follows:

$$\frac{\delta z}{2d} = \hat{C}_{z\varphi}\sqrt{\frac{2^d}{d}}\sqrt{\varphi - \varphi_j} \tag{3.13}$$

$$\delta z = 2d\hat{C}_{z\varphi}\sqrt{\frac{2^d}{d}}\sqrt{\varphi - \varphi_j}. \tag{3.14}$$

Mean Field Prediction of Packing Fraction vs Number of Excess Contacts

By combining equations 10 and 14, we can also predict the relation between δz and P:

$$\delta z = 2d\hat{C}_{z\varphi}\sqrt{\frac{2^d}{d}}\sqrt{\frac{d}{\hat{C}_{p\varphi}}P} \tag{3.15}$$

$$= 2d\hat{C}_{z\varphi}\sqrt{\frac{2^d}{\hat{C}_{p\varphi}}}\sqrt{P} \tag{3.16}$$

$$\tag{3.17}$$

where we define $\hat{C}_{zp} = \frac{2\hat{C}_{z\varphi}}{\sqrt{\hat{C}_{p\varphi}}}$.

Excess Contacts vs Excess Packing Fraction Prefactor Scaling

From eqns 5 and 6 we can simply relate δz and φ as follows:

$$\delta z = C_{z\varphi}\left(\Delta\varphi\right)^{1/2} \tag{3.18}$$

where clearly,

$$C_{z\varphi} = C_{zp}\sqrt{C_{p\varphi}}. \tag{3.19}$$

In figure 7, we show this scaling seperately for each dimension. We fit each line to eqn 3.18 to find the values of the prefactor $C_{z\varphi}$ in each dimension, the values of which are shown in the inset. These values agree well with both the mean field prediction above $3D$, shown as a black line, and our calculated value from C_{zp} and $C_{p\varphi}$, shown as black x's in figures 1 and 2.

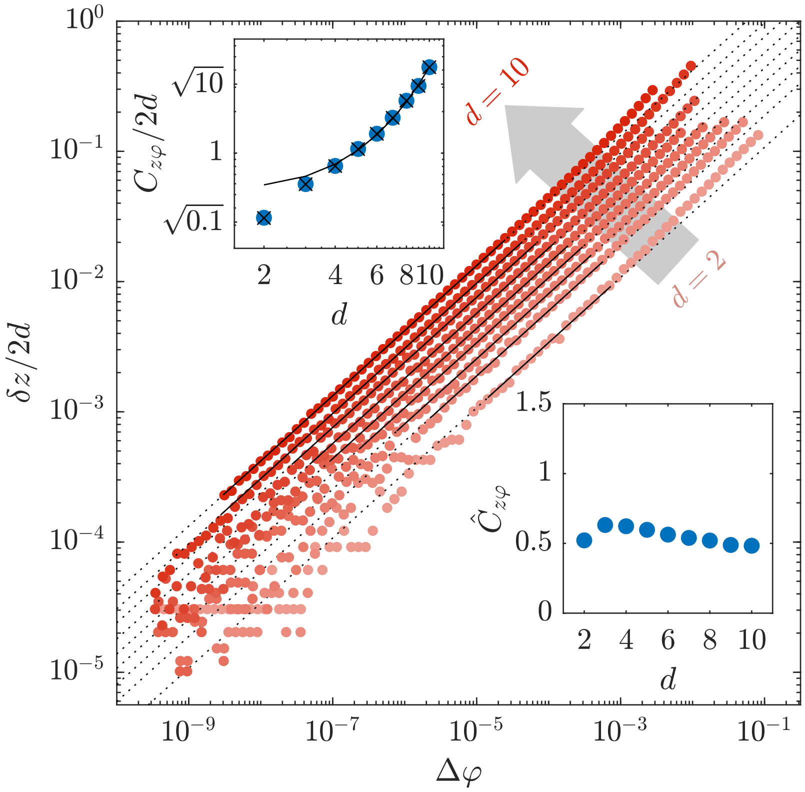

FIGURE 7. Measured excess contacts scales with the square root of excess packing fraction for systems from $d = 2$ to $d = 10$ (red circles). Black lines show the fits for C_{zp} using eqn 3.18. For our fits, we ignore data at high pressure and low contact number as in figure 2. Dotted lines show the extension of our fits beyond the fitted range. Inset shows the measured values of $C_{z\varphi}$ (blue circles), which scale in agreement with the mean field prediction eqn 3.14 using measured values of with $\hat{C}_{z\varphi} \approx 0.83$. Additionally, to note consistency we show that our measured values of $C_{z\varphi}$ agree well with values calculated from our measurements of $C_{p\varphi}$ and C_{zp} using eqn 3.19 (black x's).

Dimensional Dependence of Force Moment Ratios

In figure 8 we show that the ratio of force moments does not depend strongly on dimension. This empirical fact may seem at odds with previous reports of how the low-force part of the distribution differs from its mean-field form in low dimensions [**? ?**]. The low-force part of the distribution has $P(f) \propto f^{\theta}$, where $\theta \approx 0.17$ in $d = 2$ smoothly rises to a $d = \infty$ value of $\theta \approx 0.42$. The high-force behaviour decays like an exponential or a stretched exponential; thus, we have computed the theoretical value of this moment ratio for distributions of the form $P(f) \sim f^{\theta} e^{-f/f_0}$ and $P(f) \sim f^{\theta} e^{-f^2/f_0^2}$, as shown in figure 9. We find that neither of these assumed distributions quantitatively predicts the measured moment ratio for the known values of θ, but they do show that the known variation in θ should not make us expect a large variation in this moment ratio.

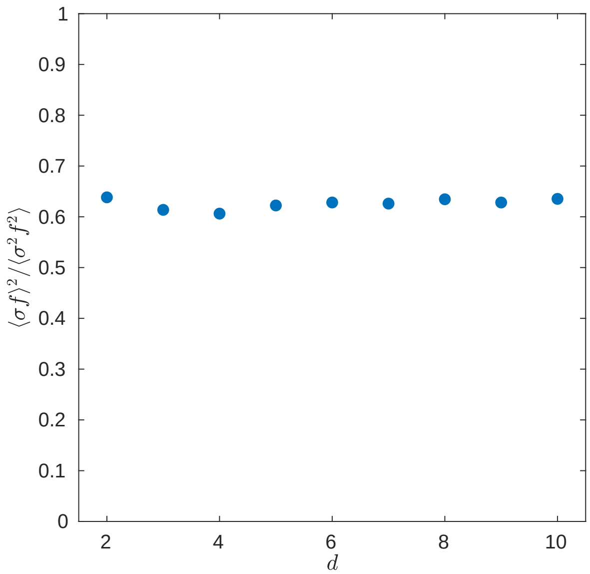

FIGURE 8. Dimensionless moment ratio of first and second moments of σf shows no dimensional dependence

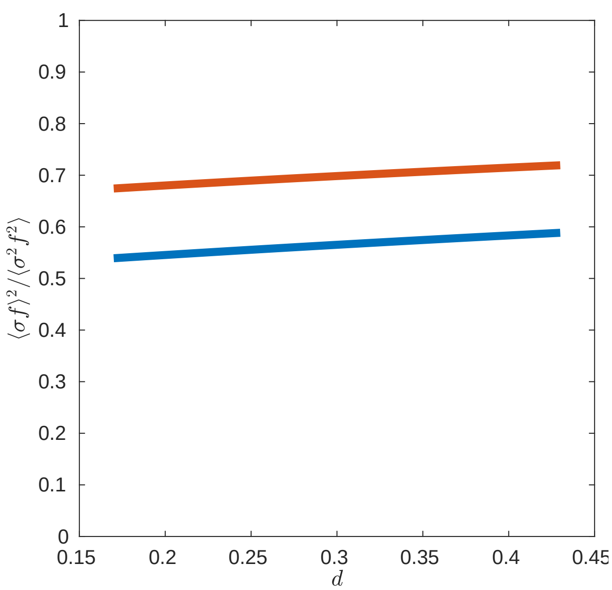

FIGURE 9. Neither the force distribution $f^\theta e^{-f/f_0}$ (blue) nor the distribution $f^\theta e^{-f^2/f_0^2}$ (red) predicts a strong θ dependence for the relevant moment ratio

Accounting for Polydispersity in Pressure vs. Packing Fraction Scaling

To account for the case with varying spring constants we also form the matrix of inverse spring constants

$$k^{-1} = \frac{1}{2\varepsilon} \begin{pmatrix} \sigma_{ij}^2 & & \\ & \ddots & \\ & & \sigma_{kl}^2 \end{pmatrix}. \tag{3.20}$$

and the projection operator onto the states of self stress

$$S = \sum_{i=1}^{N\Delta z} |s_i\rangle \langle s_i| \,. \tag{3.21}$$

In terms of these quantities, the bulk modulus may be written as [**? ? ?**]

$$\frac{\partial^2 E}{\partial V^2} = \frac{1}{V} \langle E| \, S \left(S \left(k^{-1}\right) S\right)^{-1} S \, |E\rangle \,. \tag{3.22}$$

In the one SSS approximation, we can evaluate the two projected quantities that we need to evaluate equation 3.22. Equations 10 and 12 give

$$S\,|E\rangle = \langle s_0|f\rangle \, |s_0\rangle = \frac{\langle r|f\rangle}{d\sqrt{\langle f|f\rangle}} \, |s_0\rangle = \sqrt{Z} \frac{\langle rf\rangle}{d\sqrt{\langle f^2\rangle}} \, |s_0\rangle \,, \tag{3.23}$$

and equations 3.20 and 12 give

$$Sk^{-1}S = |s_0\rangle \, \langle s_0|k^{-1}|s_0\rangle \, \langle s_0| = |s_0\rangle \, \frac{\langle \sigma^2 f^2\rangle}{2\epsilon\langle f^2\rangle} \, \langle s_0| \tag{3.24}$$

$$\left(Sk^{-1}S\right)^{-1} = |s_0\rangle \, \frac{2\epsilon\langle f^2\rangle}{\langle \sigma^2 f^2\rangle} \, \langle s_0| \tag{3.25}$$

Furthermore at lowest order in P we have $|r\rangle = |\sigma\rangle$, and we may assume $Z \approx dN$. Thus, equation 3.22 reduces to

$$K = \frac{2N\varepsilon}{dV} \frac{\langle \sigma f\rangle^2}{\langle \sigma^2 f^2\rangle}, \tag{3.26}$$

and thus via equation 9:

$$C_{p\varphi} = \frac{2}{d} \frac{\langle \sigma f\rangle^2}{\langle \sigma^2 f^2\rangle}. \tag{3.27}$$

It has recently been suggested the relationship between prestress and number of excess contacts collapses perfectly when compared across dimensions [**?**]. We define prestress e as in ref. [**?**] as:

$$e = (d-1)\left\langle \frac{-V'(r_{ij})}{r_{ij}V''(r_{ij}} \right\rangle_{ij} \tag{3.28}$$

and expected to scale as:

$$\delta z = C_{ze} e^{\frac{1}{2}} \tag{3.29}$$

because it is proportional to pressure near the jamming transition [**?**]. We examine the collapse of scaled excess contacts with prestress (fig. 11), and compare it to the collapse of excess contacts scaled by the mean field prediction with pressure (fig. 10). In figure 11 we see that the collapse with prestress is not quite perfect - there is a clear upward trend. This stands in contrast to the inset of figure 10, which shows $\hat{C}_{zp}$ to be nearly constant above three dimensions.

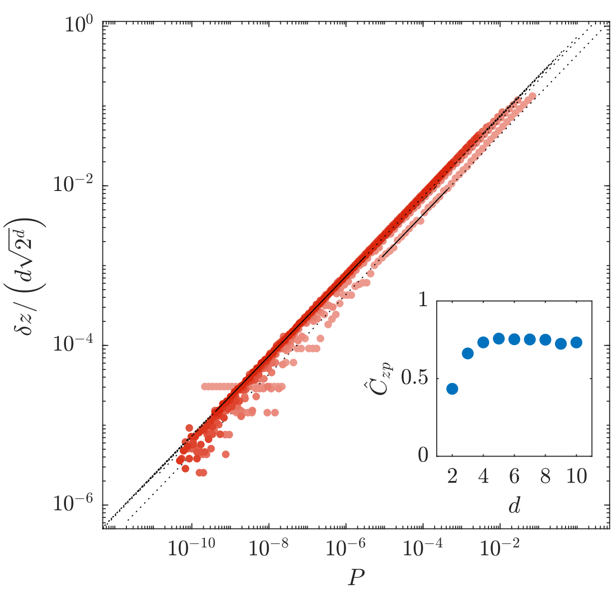

FIGURE 10. Scaled excess contacts scales with the square root of pressure as in figure 2. However, with excess contacts scaled by the expected mean field prediction, eqn. 8, the data collapse onto a single line. The inset confirms the collapse, showing $\hat{C}_{zp}$ to be nearly constant.

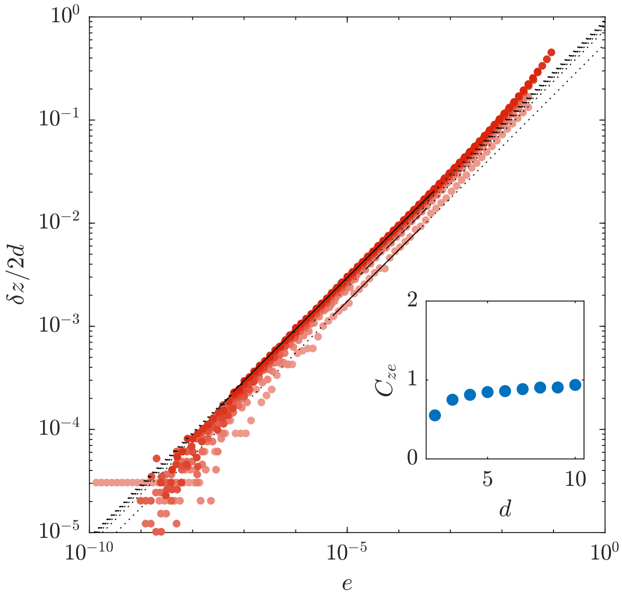

FIGURE 11. Scaled excess contacts scales with the square root of prestress for systems from $d = 2$ to $d = 10$. Black lines show the fits for C_{ze} using eqn 3.29. The fits ignore high and low pressure data as in figure 2. Lower inset shows the measured values of C_{ze} which have a clear upward trend.

In fact, close to jamming so that $r \approx \sigma$ and $Z \approx Nd$, our dimensionless pressure P as defined in equation 4 is related to the prestress by

$$P = \frac{\bar{V}_p}{\varepsilon V d} \sum_{i,j} \mathbf{f}_{ij} \cdot \mathbf{r}_{ij} \tag{3.30}$$

$$= \frac{\bar{V}_p}{\varepsilon V d} Z \langle f_{ij} r_{ij} \rangle_{ij} \tag{3.31}$$

$$= \frac{2\varphi Z}{d} \left\langle \frac{r_{ij}}{\sigma_{ij}} \left(1 - \frac{r_{ij}}{\sigma_i j} \right) \right\rangle_{ij} \tag{3.32}$$

$$= \frac{2\varphi Z}{d} \left\langle \frac{-r_{ij} V'(r_{ij})}{\sigma_{ij}^2 V''(r_{ij}} \right\rangle_{ij} \tag{3.33}$$

$$\approx 2 \frac{\varphi_{\mathrm{J}}}{d-1} e. \tag{3.34}$$

Thus, our better-fitting form for the $z - P$ relationship amounts to the statement that

$$\frac{\Delta z}{2d} = \hat{C}_{\varphi} \sqrt{\frac{d}{d-1}} \sqrt{e}. \tag{3.35}$$

Thus our scaling forms agree with the statement of reference [**?**] in the infinite-d limit, although we see better fit with our form in low dimensions.